Chronic oxidative stress promotes GADD34-mediated phosphorylation of the TAR DNA-binding protein TDP-43, a modification linked to neurodegeneration

Received for publication, August 23, 2017, and in revised form, November 1, 2017 Published, Papers in Press, November 6, 2017, DOI 10.1074/jbc.M117.814111

Catherine Wenhui Goh[‡], Irene Chengjie Lee[‡§], Jeyapriya Rajameenakshi Sundaram[‡§], Simi Elizabeth George[§], Permeen Yusoff[‡§], Matthew Hayden Brush[¶], Newman Siu Kwan Sze[‖], and Shirish Shenolikar[‡§1]**

*From the Signature Research Programs in [‡]Neuroscience and Behavioural Disorders and [§]Cardiovascular and Metabolic Disorders, Duke-NUS Medical School, Singapore 169857, Singapore, the [¶]Ontology Development group, Oregon Health and Science University, Portland, Oregon 97239, the [‖]School of Biological Sciences, Nanyang Technological University, Singapore 639798, Singapore, and the **Department of Psychiatry and Behavioral Sciences and Department of Pharmacology and Cancer Biology, Duke University School of Medicine, Durham, North Carolina 27710*

Edited by Roger J. Colbran

Oxidative and endoplasmic reticulum (ER) stresses are hallmarks of the pathophysiology of ALS and other neurodegenerative diseases. In these stresses, different kinases phosphorylate eukaryotic initiation factor eIF2α, enabling the translation of stress response genes; among these is *GADD34*, the protein product of which recruits the α-isoform of protein phosphatase 1 catalytic subunit (PP1α) and eIF2α to assemble a phosphatase complex catalyzing eIF2α dephosphorylation and resumption of protein synthesis. Aberrations in this pathway underlie the aforementioned disorders. Previous observations indicating that GADD34 is induced by arsenite, a thiol-directed oxidative stressor, in the absence of eIF2α phosphorylation suggest other roles for GADD34. Here, we report that arsenite-induced oxidative stress differs from thapsigargin- or tunicamycin-induced ER stress in promoting *GADD34* transcription and the preferential translation of its mRNA in the absence of eIF2α phosphorylation. Arsenite also stabilized GADD34 protein, slowing its degradation. In response to oxidative stress, but not ER stress, GADD34 recruited TDP-43, and enhanced cytoplasmic distribution and cysteine modifications of TDP-43 promoted its binding to GADD34. Arsenite also recruited a TDP-43 kinase, casein kinase-1ϵ (CK1ϵ), to GADD34. Concomitant with TDP-43 aggregation and proteolysis after prolonged arsenite exposure, GADD34-bound CK1ϵ catalyzed TDP-43 phosphorylations at serines 409/410, which were diminished or absent in GADD34$^{-/-}$ cells. Our findings highlight that the phosphatase regulator, GADD34, also functions as a kinase scaffold in response to chronic oxidative stress and recruits CK1ϵ and oxidized TDP-43 to facilitate its phosphorylation, as seen in TDP-43 proteinopathies.

Protein homeostasis, also referred to as proteostasis, coordinates the processes of protein synthesis, folding, and degradation that together impose a high demand on the cell's energy reserves. Thus, an unfavorable environment, such as nutrient deprivation, oxidative stress, heat shock, and radiation, negatively impacts proteostasis, and the accompanying proteotoxic stress contributes to many human diseases (1). A common cellular response to stress is the phosphorylation of the eukaryotic translational initiation factor, eIF2α, on serine 51, by one or more eIF2α kinases. This phosphorylation of eIF2α attenuates the assembly of the translational initiation complex, consisting of the ribosomal subunits and initiation factors, at AUG start sites in mRNAs and represses general protein synthesis. At the same time, P-eIF2α enhances translation of a select group of mRNAs, characterized by the presence of upstream ORFs (2–4), such as those encoding the transcription factors ATF4 and CHOP. These initiate a transcriptional program that enhances the expression of genes controlling amino acid and tRNA metabolism as well as the antioxidant response, preparing cells for the resumption of protein synthesis and ensuring cell survival (5, 6). Among the genes transcribed and translated in response to P-eIF2α is *GADD34* (growth arrest and DNA damage-inducible transcript 34, also known as *PPP1R15a*), whose protein product recruits the α-isoform of protein phosphatase 1 catalytic subunit (PP1α) and eIF2α to assemble an active eIF2α phosphatase (7). Thus, the stress-mediated induction of GADD34 functions as a feedback loop promoting eIF2α dephosphorylation and recovery from stress. The aberrant control of this integrated stress response (ISR)[2] pathway results in the accumulation of intracellular protein aggregates and programmed cell death (8), hallmarks of ALS, Alzheimer's, Huntington's, and Parkinson's diseases.

This work was supported by a Duke-NUS graduate fellowship (to C. W. G.) and Duke-NUS start-up funds provided by the Singapore Ministry of Health (to S. S.). Additional support was provided by A-Star/BMRC Translational and Clinical Research Partnership Award ACP0113683 and National Medical Research Council Translational Clinical Research Flagship Award NMRC/TCR/013-NNI/2014 (to S. S.). The authors declare that they have no conflicts of interest with the contents of this article.

This article contains Figs. S1–S4.

[1] To whom correspondence should be addressed: Signature Research Programs in Neuroscience and Behavioural Disorders and Cardiovascular and Metabolic Disorders, Duke-NUS Medical School Singapore, 8 College Rd., Singapore 169857, Singapore. E-mail: Shirish.Shenolikar@Duke-NUS.edu.sg.

[2] The abbreviations used are: ISR, integrated stress response; FCCP, carbonyl cyanide *p*-trifluoromethoxyphenylhydrazone; FTLD, frontotemporal lobar dementia; TN, tunicamycin; TG, thapsigargin; Ars, arsenite; MEF, mouse embryo fibroblast; P-eIF2α, phosphorylated eIF2α; CHX, cycloheximide; HMW, high-molecular weight; RIPA, radioimmune precipitation assay; MEM, minimal essential medium; CFTR, cystic fibrosis transmembrane conductance regulator; WCL, whole-cell lysate; FA, formic acid; IP, immunoprecipitate(s).

The loss of mouse genes encoding GADD34 and its structural homologue, CReP (constitutive repressor of eIF2α phosphorylation or *PPP1R15b*), eliminates all eIF2α phosphatase activity and yields no embryos (9). However, crossing the *PPP1R15a/b* heterozygous mice with animals carrying a mutation (S51A) that mimics eIF2α dephosphorylation yields live pups, although they fail to thrive after birth (9). These data argued that GADD34 (and CReP) functions primarily if not exclusively as a component of eIF2α phosphatase during mouse development.

Earlier observations that GADD34 was induced by arsenite, a thiol-directed oxidative stress, in the absence of eIF2α phosphorylation (10) suggested that GADD34 served other role(s) in these stressed cells besides functioning as an eIF2α phosphatase. The apparent molecular size of the major cellular GADD34 complex at ~670 kDa (11) was also significantly larger than the eIF2α phosphatase complex, comprising GADD34, PP1α, and eIF2α. This suggested that cells contained other GADD34-interacting proteins that may also modulate the stress response. Together, these observations prompted us to initiate proteomics studies to identify novel GADD34-interacting proteins and examine their role in the cellular response to oxidative stress. Here, we report the identification of TAR DNA-binding protein (TDP-43), a known regulator of RNA and protein homeostasis (12, 13) and a major component of stress granules (14, 15), as a novel GADD34-interacting protein. Our studies showed that GADD34 recruits TDP-43 and casein kinase-1ϵ in response to arsenite and promotes TDP-43 phosphorylation at serines 409/410, modifications observed in post-mortem brains of patients with ALS and frontotemporal lobar dementia (FTLD) (16, 17). Most importantly, our data highlight the ability of GADD34, a known phosphatase regulator, to function as a kinase scaffold that controls TPD-43 phosphorylation and potentially contributes to the pathobiology of ALS and other neurodegenerative diseases.

Results

Oxidative stress induces high GADD34 levels

Our prior studies identified arsenite as among the most robust inducers of GADD34 protein in mammalian cells (10). To compare stresses, HEK293T cells were exposed to tunicamycin (TN), an inhibitor of protein glycosylation in the ER; thapsigargin (TG), which depletes ER calcium and impairs chaperone function; and arsenite (Ars), an inducer of oxidative stress. All three stresses elevated eIF2α phosphorylation in a time-dependent manner, with TN displaying the slowest onset. Whereas both TG and Ars elicited robust eIF2α phosphorylation, GADD34 accumulation was much higher in the arsenite-treated cells. Lower or no GADD34 was observed in TG- and TN-treated cells over a similar time period (Fig. 1*A*). The increases in GADD34 protein mirrored stress-induced GADD34 mRNA levels, which were also the highest in arsenite-treated cells (Fig. 1*A*).

The phosphorylation of eIF2α plays an essential role in GADD34 expression in response to TG or TN, such that the knock-in substitution of serine 51 with alanine (S51A), which abolishes eIF2α phosphorylation, also eliminates GADD34 expression in response to TG and TN (18). These studies were also the first to note, however, that arsenite still induced GADD34 expression in the eIF2α (S51A) mouse embryonic fibroblasts (MEFs), but the underlying mechanisms were not investigated. Our previous studies showed that TG treatment of WT MEFs resulted in transient increase in eIF2α phosphorylation, reaching a peak at 30 min (19). The current studies showed that at 1–2 h, P-eIF2α levels subsided with the expression of GADD34 (Fig. 1*B*). The P-eIF2α-mediated activation of ISR was demonstrated by the time-dependent increases in mRNAs and proteins representing CHOP and GADD34, downstream ISR genes. The ablation of eIF2α phosphorylation in S51A MEFs, however, strongly suppressed the TG-mediated induction of CHOP and GADD34 proteins and mRNAs, as well as the mRNA encoding ATF4, another ISR gene that is essential for GADD34 transcription (20). In sharp contrast, arsenite induced GADD34 protein expression in both WT and S51A MEFs (Fig. 1*C*). Arsenite also increased the levels of mRNAs encoding GADD34, CHOP, and ATF4, in both WT and S51A MEFs. Despite the increase in CHOP mRNA, no CHOP protein was detected in S51A MEFs, potentially highlighting that efficient translation of CHOP mRNA requires eIF2α phosphorylation (3). This was surprising, as the GADD34 mRNA, which also contains upstream ORFs that enable its translation in the presence of P-eIF2α (1), was efficiently translated in the S51A MEFs.

During cell recovery from stress, the GADD34 protein undergoes rapid proteasomal degradation, displaying a half-life of <1 h (10). To assess the impact of stress on protein turnover, endogenous GADD34 protein was expressed in HEK293T cells by exposure to TG or Ars (Fig. 1*D*). The addition of cycloheximide (CHX) that inhibited new protein synthesis resulted in the rapid decay of the GADD34 protein in TG-treated cells, with rates similar to those seen in control unstressed cells (Fig. 1*E*), and little or no GADD34 protein was visible after 2 h. By contrast, the decay rate for GADD34 in arsenite-treated cells was slower, with GADD34 protein still visible at 4 h. To strengthen these initial observations, we coexpressed human GADD34-GFP, shown to degrade at a rate similar to that of endogenous GADD34 (10), along with the proteasome substrate, GFPu (21), as an independent readout of proteasome function. Both GADD34-GFP and GFPu were rapidly degraded in control CHX-treated cells (Fig. 1*E*). The addition of MG132, a proteasomal inhibitor, attenuated the turnover of both GADD34-GFP and GFPu, consistent with their degradation by the proteasome. Whereas TG had no discernible effect on turnover of GADD34-GFP or GFPu, arsenite significantly stabilized GADD34-GFP without affecting the degradation of GFPu. These data showed that arsenite preferentially stabilized GADD34-GFP without impairing proteasomal function. Thus, the combined effects of increased transcription, translation, and protein stability accounted for the high GADD34 levels seen in cells undergoing oxidative stress.

Oxidative stress enhances GADD34 binding to TDP-43

To identify novel GADD34 functions, we expressed FLAG-GADD34 in HEK293T cells and subjected anti-FLAG immunoprecipitates to mass spectrometry. In six independent experi-

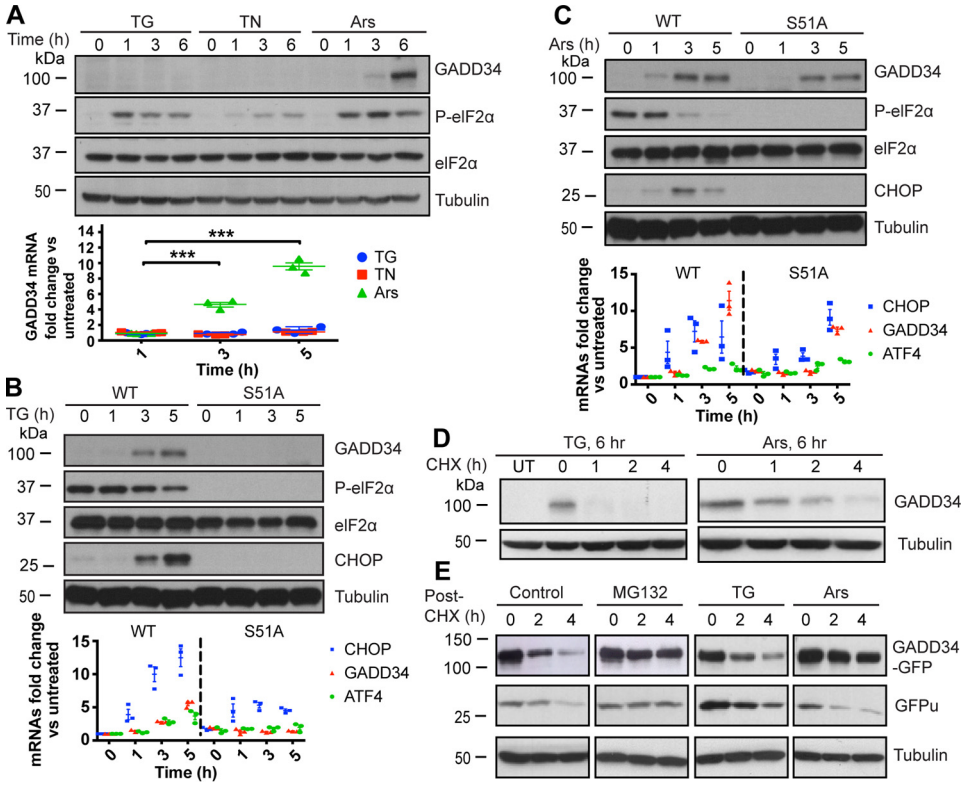

Figure 1. Arsenite induces high levels of GADD34. *A*, the *top panel* shows the time-dependent changes in P-eIF2α and GADD34 monitored by immunoblotting following the exposure of HEK293T cells to TG (5 μM), TN (10 μg/ml), and Ars (100 μM), as described under "Materials and methods." Immunoblotting for total eIF2α and tubulin were undertaken to display equal protein loading. Representative immunoblots from three independent experiments ($n = 3$) are shown. The *bottom panel* displays the scatter plot of GADD34 mRNA levels in the same cells using RT-PCR (representative data from two independent experiments ($n = 2$), each undertaken in triplicate are shown with S.E. (*error bars*)). ***, $p < 0.001$. *B* and *C*, ER stress signaling in WT and eIF2α (S51A) MEFs treated with TG (*B*) and Ars (*C*) was monitored by changes in P-eIF2α. Expression of the downstream proteins, GADD34 and CHOP (*top panels*) and mRNAs encoding ATF4 (*circles*), CHOP (*squares*), and GADD34 (*triangles*) are also shown as scatter plots (*bottom panels*). Tubulin was monitored as a protein loading control. Representative immunoblots and scatter plots from three independent experiments ($n = 3$) are shown. *D*, HEK293T cells, treated with TG or Ars for 6 h to induce endogenous GADD34; protein levels following the addition of CHX were monitored by immunoblotting with anti-GADD34 antibody. Immunoblotting for tubulin displayed equal protein loading. Representative data from five independent experiments ($n = 5$) are shown. *E*, GADD34-GFP and GFPu proteins were expressed in HEK293T cells, either control or treated with MG132, TG, or Ars and monitored following the addition of CHX. Tubulin immunoblotting shows equivalent protein loading. Representative blots from four independent experiments ($n = 4$) are shown.

ments (the data are available at www.ebi.ac.uk/intact/ or http://www.imexconsortium.org with the identifier IM-23248), PP1α (5 of 6 experiments)[3] and eIF2α (4 of 6 experiments) were consistently identified, confirming GADD34's known ability to scaffold these two proteins (7, 22).

Among the new potential GADD34-interacting proteins identified by mass spectrometry (4 of 6 experiments) was the transactive response DNA-binding protein of 43 kDa (TDP-43), which has been implicated in RNA and protein homeostasis (13) and is present in protein inclusions in brains and spinal cords of patients with ALS and other neurodegenerative disorders (23, 24). We confirmed the association of endogenous TDP-43 using immunoblotting of anti-FLAG immunoprecipitates from FLAG-GADD34–expressing HEK293T cells with an anti-TDP-43 antibody (Fig. 2*A*). KARA, a mutant GADD34 that does not bind PP1α (22), showed similar TDP-43 binding to WT FLAG-GADD34, suggesting that TDP-43 binding was independent of PP1α. To examine TDP-43 association with endogenous GADD34, HEK293T cells were treated with arsenite (100 μM, 6 h) to induce GADD34 expression, and anti-TDP-43 immunoprecipitates were immunoblotted with an anti-GADD34 antibody. These data showed that endogenous GADD34 bound the endogenous TDP-43 with an efficacy similar to that of the known TDP-43–interacting RNA-binding protein, TIAR (Fig. 2*B*). A faint band representing TDP-43 was seen in immunoprecipitates using control or nonspecific IgG. This probably represented arsenite-induced TDP-43–containing protein aggregates, which cosedimented with the IgG-bound protein G beads. These samples, however, contained no GADD34 or TIAR, highlighting the specificity of the anti-TDP-43 immunoprecipitates. In these experiments, we were unable to detect TDP-43 in the reciprocal anti-GADD34 immunoprecipitates that had been shown previously to contain PP1α and eIF2α. This suggested that the TDP-43 footprint on GADD34 was different from that of PP1α or eIF2α such that TDP-43 association occluded the binding of GADD34 by the anti-GADD34 antibody, whose epitope resided near the C terminus of human GADD34.

To examine the potential modulation of GADD34/TDP-43 binding by stress, FLAG-GADD34-expressing HEK293T cells were exposed to various stresses, and FLAG-GADD34 immunoprecipitates were analyzed by immunoblotting with anti-TDP-43 (Fig. 3*A*). These data showed that arsenite, and to a

[3] Please note that the JBC is not responsible for the long-term archiving and maintenance of this site or any other third party hosted site.

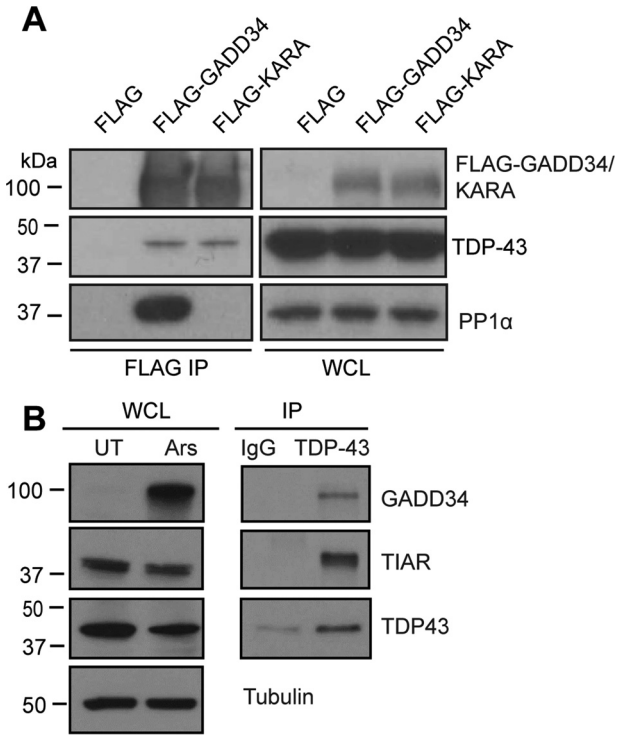

Figure 2. GADD34 binds TDP-43. *A*, anti-FLAG immunoprecipitates (*FLAG IP*) from HEK-293 cells expressing either WT FLAG-GADD34 or the PP1-binding deficient GADD34 mutant (KARA) showed the presence of equivalent endogenous TDP-43. Levels of FLAG-GADD34 proteins, TDP-43, and PP1α in WCL are also shown by immunoblotting. Representative data from three independent experiments ($n = 3$) are shown. *B*, immunoprecipitation with an anti-TDP-43 antibody demonstrated the comparable avidity of TDP-43 for endogenous GADD34 induced by arsenite exposure (100 μM, 6 h) and TIAR, a known TDP-43–binding protein. The cellular content of GADD34, TIAR, and TDP-43 (WCL) are also shown by immunoblotting with the respective antibodies. Representative data from three independent experiments are shown ($n = 3$).

lesser extent, FCCP, a mitochondrial inhibitor, enhanced GADD34 binding to TDP-43. Exposure to increasing arsenite concentrations highlighted a dose dependence for FLAG-GADD34 binding to endogenous TDP-43 (also to a lesser extent to eIF2α), although PP1α binding to GADD34 was independent of stress (Fig. 3*B*). *N*-Acetylcysteine, an antioxidant, inhibited the arsenite-induced GADD34/TDP-43 association (Fig. 3*C*), illustrating that an oxidative stress was elicited by arsenite that enhanced TDP-43 recruitment to the GADD34·PP1α·eIF2α complex.

Ectopically expressed GADD34 strongly suppresses stress signaling (25). Thus, to examine the importance of P-eIF2α in GADD34/TDP-43 association, low levels of FLAG-GADD34 were expressed in WT and S51A MEFs (Fig. 3*D*). As anticipated, a short exposure to arsenite increased eIF2α phosphorylation in WT MEFs but not in S51A MEFs. Arsenite partially reduced the TDP-43 levels in both cells, possibly redirecting the protein to TDP-43–containing stress granules (14) or to detergent-insoluble protein inclusions (25, 26). Regardless, the anti-FLAG immunoprecipitates from both arsenite-treated WT and S51A MEFs contained detectable TDP-43. These data showed that GADD34/TDP-43 association was independent of P-eIF2α and ISR signaling.

Molecular determinants in GADD34 that mediate TDP-43 binding

Co-immunoprecipitation of TDP-43 from arsenite-treated HEK293T cells expressing FLAG-GADD34 polypeptides showed that other than the peptide encompassing the N-terminal region, amino acids 1–200, all other GADD34 polypeptides bound TDP-43 (Fig. 4, *A* and *B*). By comparison, only the C-terminal domain of GADD34, represented by amino acids 514–674, bound PP1α (22). Purified recombinant GST-GADD34 proteins also sedimented TDP-43 as well as PP1α and eIF2α from HEK293T lysates (Fig. 4*C*). These *in vitro* experiments confirmed that the C-terminal region, 514–674, bound PP1α and eIF2α although much more weakly. By comparison, the N-terminal domain, 1–513, bound eIF2α avidly but did not interact with PP1α (7). The full-length GST-GADD34, 1–674, and the C-terminal peptide, 241–674, expressed poorly in bacteria and, thus, showed a reduced binding to eIF2α, PP1α, and TDP-43 (Fig. 4*C*). Together, these experiments suggested that an extended region of GADD34 represented the TDP-43–docking site (Fig. 4*A*) that still accommodated eIF2α and PP1α binding to GADD34.

Cytoplasmic redistribution and cysteine modification of TDP-43 facilitate GADD34 binding

Arsenite promotes the oxidation of one or more cysteines in TDP-43 (26), and these modifications have been implicated in TDP-43 redistribution to the cytoplasm and incorporation into protein inclusions and stress granules (15). To assess the role of cysteine oxidation and nucleocytoplasmic shuttling of TDP-43 in GADD34 binding, Myc-TDP-43 proteins with the substitutions C173S, C175S, C198S, and C244S, termed 4CS, or lacking two nuclear localization sequences (ΔNLS12) or one of two putative nuclear export sequences (ΔNES1) (Fig. 5*A*) were expressed in HeLa cells. Confocal microscopy of cells immunostained with anti-Myc antibody showed that WT TDP-43 was exclusively nuclear in control cells but redistributed to form cytoplasmic puncta following arsenite treatment (Fig. 5*B*). By comparison, 4CS was predominantly seen in cytosolic puncta, although 4CS-containing nuclear puncta were also seen in both control and arsenite-treated HeLa cells (Fig. 5*B*). As anticipated, ΔNLS12 was predominantly cytoplasmic, and ΔNES1 was largely nuclear. Arsenite had no apparent impact on the subcellular distribution of these mutant proteins, although nuclear puncta were seen in arsenite-treated ΔNES1-expressing cells.

Analysis of anti-Myc immunoprecipitates showed that neither cytoplasmic ΔNLS12 nor the predominantly nuclear ΔNES1 bound GADD34 in control cells, but like WT TDP-43, the binding of these mutant TDP-43 proteins to FLAG-GADD34 was enhanced by arsenite. It should be stated that ΔNES1 still retains one of the two putative nuclear export signals and, while appearing predominantly nuclear, may still traffic to the cytoplasm in response to oxidative stress. The most remarkable observation was that 4CS bound GADD34 avidly, in the presence or absence of arsenite

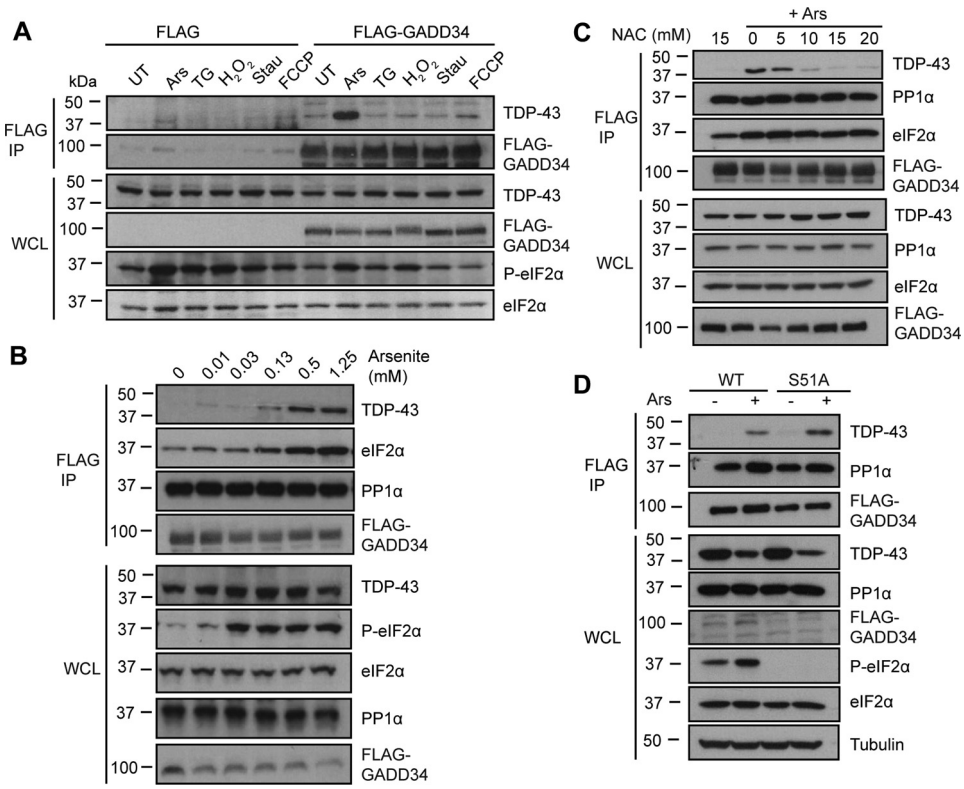

Figure 3. Oxidative stress enhances GADD34 binding to TDP-43. *A*, FLAG-GADD34-expressing HEK293T cells were subjected to various stresses (Ars (0.5 mM for 1 h), TG (1 μM for 2 h), H_2O_2 (1 mM for 2 h), staurosporine (*Stau*; 0.5 μg/ml for 2 h), FCCP (1 μM for 1 h), or MG132 (1 μM for 4.5 h)), followed by immunoprecipitation using anti-FLAG antibody. Immunoprecipitates (IP) and WCL were immunoblotted with anti-TDP-43 and anti-FLAG antibodies. P-eIF2α and eIF2α in WCL were also analyzed. Representative data from three independent experiments ($n = 3$) are shown. *B*, FLAG-GADD34-expressing HEK293T cells were treated with increasing doses of Ars for 1 h and subjected to immunoprecipitation with anti-FLAG antibody. IP and WCL were immunoblotted for TDP-43, eIF2α, PP1α, and FLAG-GADD34. P-eIF2α was also monitored in WCL. Representative data from four independent experiments ($n = 4$) are shown. *C*, FLAG-GADD34–expressing HEK293T cells were pretreated with increasing concentrations of *N*-acetylcysteine for 1 h, followed by Ars (0.5 mM, 1 h) and subjected to immunoprecipitation with anti-FLAG. IP and WCL were analyzed for TDP-43, PP1α, eIF2α, and FLAG-GADD34 by immunoblotting. Representative data from two independent experiments ($n = 2$) are shown. *D*, FLAG-GADD34 was expressed in WT or S51A MEFs, which were then exposed to Ars (0.5 mM, 1 h). Following immunoprecipitation with anti-FLAG antibody, the content of TDP-43, PP1α, and FLAG-GADD34 in IP and WCL from cells treated with and without arsenite was assessed by immunoblotting. P-eIF2α and tubulin were also monitored in WCL. Representative data from two independent experiments ($n = 2$) are shown.

(Fig. 5*C*). These data suggested that whereas the cytoplasmic localization of TDP-43 was important, by itself, it was insufficient for GADD34 binding, and the cysteine oxidation of TDP-43 following oxidative stress was equally critical for GADD34 association.

To investigate the importance of cysteine modifications in recruitment of other TDP-43 targets, WT Myc-TDP-43 or Myc-4CS was coexpressed with FLAG-GADD34 in HEK293T cells. Analysis of anti-Myc immunoprecipitates confirmed that arsenite enhanced the recruitment of WT Myc-TDP-43 to FLAG-GADD34 and that Myc-4CS binding to FLAG-GADD34 was insensitive to arsenite (Fig. 5*D*). By contrast, the association of another TDP-43–binding protein, TIAR, to both WT Myc-TDP-43 and Myc-4CS showed a strict requirement for arsenite. These data (Fig. 5*E*) highlighted the selectivity of the cysteine modifications on TDP-43 for GADD34 recruitment.

Cytoplasmic TDP-43 (4CS) aggregates are phosphorylated at serines 409 and 410

Oxidation of TDP-43 results in high-molecular weight (HMW) TDP-43–containing complexes, seen on polyacrylamide gel electrophoresis in non-reducing conditions (26). We utilized a biochemical protocol (15) to extract soluble proteins using RIPA buffer and subsequently solubilizing the protein aggregates with urea. Arsenite treatment of HEK293T cells expressing WT Myc-TDP-43 showed that Myc-TDP-43 levels gradually decreased in the RIPA-soluble fraction, representing largely cytosol, as judged by the presence of the cytoplasmic protein GAPDH. Moreover, there was parallel accumulation of Myc-TDP-43 seen in the urea-soluble fraction. The urea fraction displayed multiple slowly migrating HMW bands, representing Myc-TDP-43–containing aggregates, that could be resolved by electrophoresis on non-reducing gels. These aggregates displayed no immunoreactivity with an anti-phospho-TDP-43 antibody (Fig. 6*A*), and there was also no detectable phosphorylation of WT Myc-TDP-43 in the RIPA-soluble fraction. In contrast to WT Myc-TDP-43, the urea-soluble fraction containing Myc-4CS was devoid of HMW complexes and showed a robust and time-dependent phosphorylation at serines 409 and 410, modifications first identified in patients with TDP-43 proteinopathies (16, 17). These data suggested that the cysteine oxidations in TDP-43 not only promoted its cytoplasmic localization and binding to GADD34 but also enhanced TDP-43 phosphorylation in the urea-soluble protein inclusions.

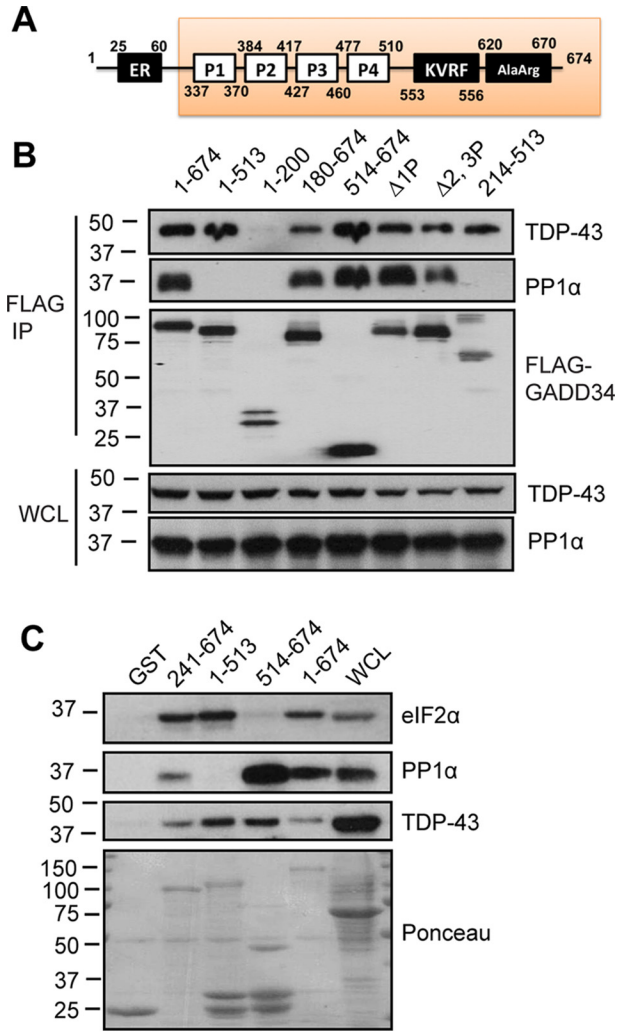

Figure 4. TDP-43 interacts with an extended region of GADD34. *A*, the schematic shows functional domains defined in GADD34, namely the endoplasmic reticulum localization domain (*ER*), the PEST repeats (*P1–P4*), and two PP1α-binding sequences (KVRF and Arg-Ala repeats). The *shaded box* highlights the region of GADD34 that associates with TDP-43 as shown in the experiments undertaken in *B* and *C*. *B*, FLAG-GADD34 polypeptides, identified by the amino acid numbers, were expressed in HEK293T cells and, following arsenite exposure, were immunoprecipitated with anti-FLAG. In addition to the FLAG-GADD34 peptides in the IP, IP and WCL were immunoblotted for TDP-43 and PP1α. Representative data from three independent experiments ($n = 3$) are shown. *C*, HEK293T cell lysates were incubated with recombinant GST-GADD34 polypeptides, listed by amino acid numbers, bound to GSH-Sepharose. Following the sedimentation of the affinity beads and their washing as described under "Materials and methods," the GST-GADD34–bound proteins, eluted as described under "Materials and methods," and WCL were immunoblotted for eIF2α, PP1α, and TDP-43. The GST-GADD34 proteins were visualized by staining with Ponceau dye. Representative data from three independent experiments ($n = 3$) using at least two biological replicates are shown.

Immunostaining of Myc-4CS–expressing HeLa cells with the anti-phospho-TDP-43 (Ser-409/410) antibody following arsenite exposure confirmed the presence of cytoplasmic phospho-4CS–containing protein inclusions (Fig. 6*B*). Their lack of co-staining by an anti-TIAR antibody demonstrated that these puncta were not stress granules. By contrast, cells expressing WT Myc-TDP-43 possessed smaller cytoplasmic puncta, following arsenite exposure, which displayed TIAR immunoreactivity, identifying these as stress granules (Fig. 6*B*), and no phospho-TDP-43–positive protein aggregates were seen in cells that expressed WT Myc-TDP-43.

Prolonged oxidative exposure promotes WT TDP-43 phosphorylation at serines 409/410

To assess whether WT TDP-43 was simply immune to phosphorylation or its covalent modification was significantly slower than that seen for 4CS, we treated WT Myc-TDP-43–expressing HEK293T cells with arsenite for longer periods, up to 24 h, during which we observed a time-dependent increase in cellular GADD34. This endogenous GADD34 was observed in both the RIPA-soluble and urea-soluble fractions, suggesting that chronic or prolonged oxidative stress recruited GADD34 to the TDP-43–containing aggregates solubilized by urea (Fig. 6*C*). Interestingly, another GADD34-interacting protein identified by mass spectrometry, casein kinase-1ϵ (CK1ϵ), a candidate TDP-43 (serines 409/410) kinase (16, 27), showed a time-dependent decrease in the RIPA fraction with a concomitant increase in the urea-soluble fraction, similar to GADD34 and WT TDP-43 (Fig. 6, *A* and *C*). In parallel with the accumulation of GADD34, Myc-TDP-43, and CK1ϵ in the urea-soluble fraction, there was a notable reduction in the Myc-TDP-43–containing HMW species and increasing proteolysis of Myc-TDP-43 to a 35-kDa peptide fragment seen in brains of ALS patients (23, 28). However, the more remarkable observation was that in response to prolonged arsenite exposure, WT Myc-TDP-43 that accumulated in the urea-soluble fraction was phosphorylated at serines 409/410. These data were supported by confocal microscopy of the Myc-TDP-43–expressing HeLa cells that noted the appearance of cytoplasmic phospho-TDP-43–containing protein aggregates in cells treated with 100 μM arsenite for 5 h. These puncta became even more prominent and intensely stained by anti-phospho-TDP-43 antibody after 21 h of arsenite exposure (Fig. 6*D*). Attempts to show the presence of GADD34 in these phospho-TDP-43–containing aggregates by immunostaining with an anti-GADD34 antibody were unsuccessful, reemphasizing that the presence of TDP-43 appears to occlude GADD34 binding by the anti-GADD34 antibody.

GADD34 promotes oxidative stress-induced phosphorylation of endogenous TDP-43 (serines 409/410)

To establish the importance of GADD34 in the phosphorylation and aggregation of endogenous TDP-43, we analyzed WT and GADD34$^{-/-}$ MEFs that were treated with 100 μM arsenite for 5 h. Arsenite increased endogenous GADD34 levels in the RIPA-soluble fraction in WT but not GADD34$^{-/-}$ MEFs. In parallel, there was a progressive loss of endogenous TDP-43 in the RIPA-soluble fraction. Most importantly, TDP-43 gradually accumulated in the urea-soluble fraction from both WT and GADD34$^{-/-}$ cells. However, GADD34 and CK1ϵ were only present in the TDP-43–containing aggregates in WT MEFs, and consistent with this, TDP-43 was increasingly phosphorylated. As neither GADD34 nor CK1ϵ were present in the urea-soluble fraction from arsenite-treated GADD34$^{-/-}$ MEFs, no detectable TDP-43 phosphorylation occurred in these cells (Fig. 7*A*). These data emphasized the pivotal role played by arsenite-induced recruitment of

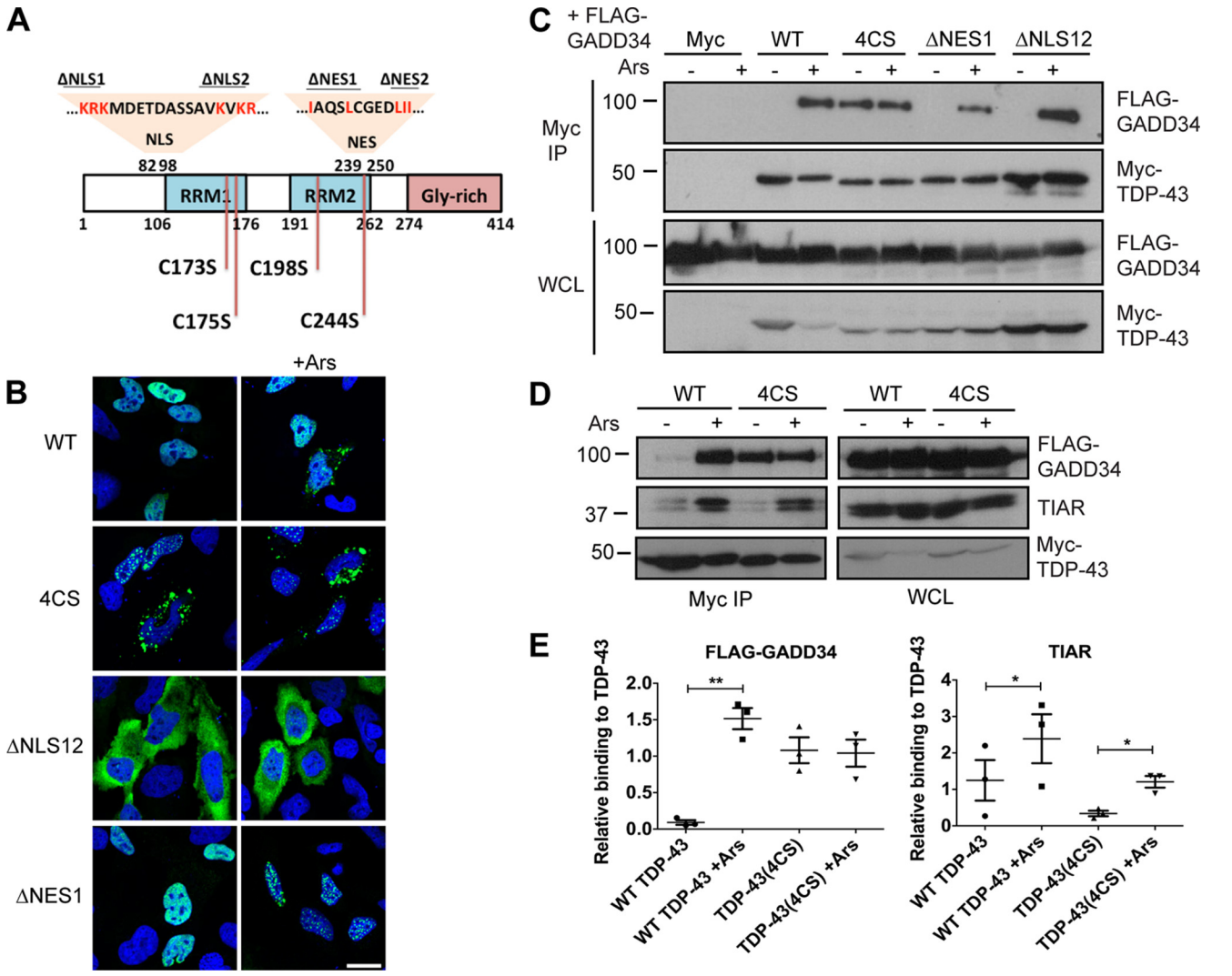

Figure 5. Cytoplasmic localization and cysteine oxidation of TDP-43 facilitates GADD34 binding. *A*, the schematic illustrates the functional domains in TDP-43, which include the two RNA-binding domains RRM1 and RRM2 and the C-terminal glycine-rich domain implicated in TDP-43 aggregation. The four cysteines oxidized in TDP-43 were substituted with serines, and the nuclear localization signals (*NLS1* and *NLS2*) and nuclear export signals (*NES1* and *NES2*) are shown with the amino acids substituted to generate ΔNLS12 and ΔNES1 in *boldface type*. *B*, the subcellular distribution of WT Myc-TDP-43, Myc-4CS, Myc-ΔNLS12, and Myc-ΔNES1 expressed in HeLa cells and stained with anti-Myc antibody is shown in *green*, with the *blue color* showing nuclear staining with Hoechst dye in cells before and after Ars (0.5 mM, 1 h) exposure. Representative data from three independent analyses ($n = 3$) are shown. *C*, WT Myc-TDP-43, 4CS, ΔNLS12, and ΔNES1 were co-expressed with FLAG-GADD34 in HEK293T cells, and anti-Myc immunoprecipitates (*Myc IP*) and WCL were analyzed for the presence of FLAG-GADD34 and Myc-TDP-43 by immunoblotting. Representative data from two independent experiments ($n = 2$) are shown. *D* and *E*, immunoprecipitation of Myc-TDP-43 and Myc-4CS from HEK293T cells either untreated (−) or Ars-treated (0.5 mM, 1 h) using anti-Myc antibody (*Myc IP*). Immunoblotting analysis of WCL revealed the levels of FLAG-GADD34, TIAR, and Myc-TDP-43 (*D*). Quantitation of endogenous TIAR and FLAG-GADD34 binding to Myc-TDP-43 or Myc-4CS either in the absence or presence of Ars is shown as a scatter plot of three independent experiments (*E*, $n = 3$), with *error bars* showing S.E. **, $p < 0.01$; *, $p < 0.05$.

GADD34 and CK1ϵ to the TDP-43–containing aggregates in TDP-43 phosphorylation at serines 409/410.

CK1 and CK2 have both been implicated in TDP-43 phosphorylation and aggregation (27, 29, 30). Moreover, our mass spectrometry studies had identified both CK1ϵ and CK2α in the anti-FLAG-GADD34 immunoprecipitates (4 of 6 experiments). Thus, we re-examined the anti-FLAG immunoprecipitates from FLAG-GADD34–expressing HEK293T cells and confirmed the CK1ϵ association with GADD34 following arsenite exposure (Fig. 7*B*). However, no detectable CK2α was seen in these immunoprecipitates, with or without arsenite. Finally the phosphorylation of WT TDP-43 in the urea-soluble fraction that resulted from prolonged arsenite exposure of HEK293T cells was significantly reduced in the presence of PF670462, a selective CK1δ/ϵ inhibitor (Fig. 7*C*), confirming the importance of GADD34-mediated scaffolding of CK1ϵ in the arsenite-induced TDP-43 phosphorylation.

Discussion

Oxidative stress is a major culprit in ALS, the most common human motor neuron disease, with over 150 mutations identified in superoxide dismutase 1 (SOD1) (31). Whereas most ALS cases are sporadic and do not possess SOD1 mutations, sporadic and familial ALS are clinically indistinguishable, hinting at a common basis for the motor neuron disease. Indeed, ubiquitin-positive cytoplasmic protein inclusions are observed in the degenerating motor neurons in both sporadic and familial ALS, pointing to defects in proteostasis. Moreover, TDP-43, a

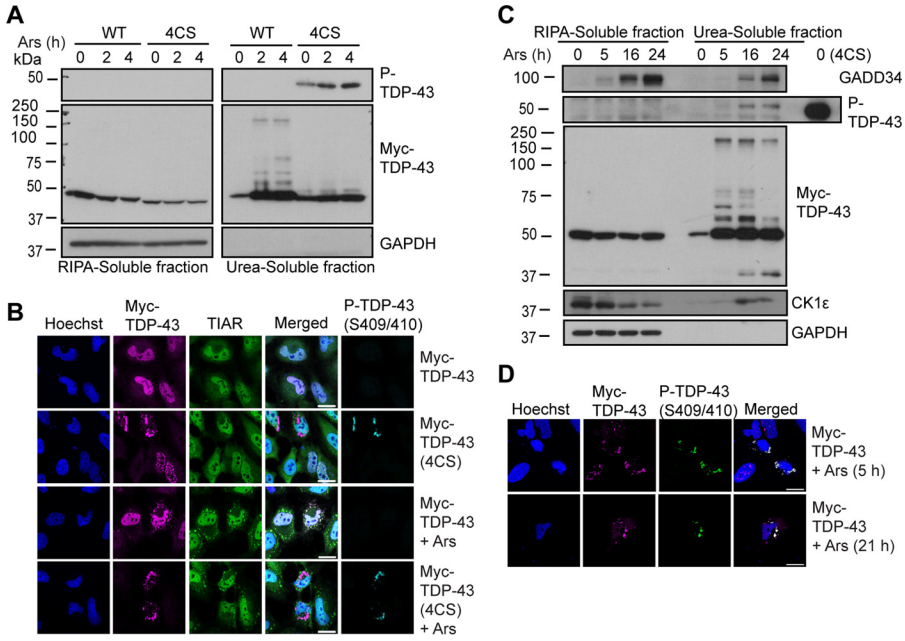

Figure 6. Chronic arsenite exposure promotes TDP-43 aggregation and phosphorylation at Ser-409/410. *A*, HEK293T cells expressing either WT Myc-TDP-43 or Myc-4CS were treated with Ars (100 μM from 0–4 h) and fractionated into RIPA-soluble and urea-soluble fractions, which were analyzed for P-TDP-43, Myc-TDP-43, or Myc-4CS and GAPDH by immunoblotting. Representative data from three independent experiments ($n = 3$) are shown. *B*, HeLa cells expressing Myc-TDP-43 or Myc-4CS, either untreated or following treatment with Ars (0.5 mM, 1 h), were immunostained for TIAR, Myc-TDP-43, and P-TDP-43. Hoechst stain identified the nuclei (*blue*), shown along with staining with anti-Myc (*magenta*) and anti-TIAR (*green*) individually as well as in the *merged images*. Staining with anti-P-TDP-43 (Ser-409/410) is shown in *cyan*. *Scale bar*, 20 μM. Representative data from three independent experiments ($n = 3$) are shown. *C*, HEK293T cells expressing Myc-TDP-43, treated with Ars (100 μM, 0–24 h), were fractionated into RIPA-soluble and urea-soluble fractions, which were immunoblotted for GADD34, P-TDP-43, Myc-TDP-43, CK1ϵ, and GAPDH. The urea-soluble fraction from HEK293T cells expressing Myc-4CS was used as a positive control for P-TDP-43. Representative data from three independent experiments ($n = 3$) are shown. *D*, HeLa cells expressing Myc-TDP-43 treated with Ars (100 μM, 5 and 21 h) were immunostained for Myc-TDP-43, TIAR, and anti-P-TDP-43 (Ser-409/410). *Merged images* are shown. *Scale bar*, 20 μM. Representative data from two independent experiments ($n = 2$) are shown.

RNA-binding protein, is a major component of protein aggregates found in the post-mortem brain tissue in 97% of sporadic ALS and 45% of FTLD (23, 24). The subsequent discovery of TDP-43 mutations in familial ALS and FTLD hinted at deficits in TDP-43 function as an alternative trigger for ALS. As TDP-43 regulates cellular SOD1 levels (32), this forged a link between oxidative stress, proteotoxicity, and aberrant TDP-43 function in the pathogenesis of ALS. TDP-43-containing aggregates, increased TDP-43 phosphorylation, and caspase-mediated cleavage of TDP-43 (33) have all been linked to Alzheimer's disease and Lewy body dementias, including Parkinson's disease (28, 34) and Huntington's disease (35).

The current work showed that oxidative stress elicited by arsenite results in higher GADD34 levels than ER stress, induced by TG or TN. Our experiments extended the prior observation (36) that arsenite differs from TG in promoting GADD34 expression in the absence of P-eIF2α to show that arsenite promotes robust transcription and translation of GADD34 in S51A MEFs. Taken together with our finding that arsenite inhibited the GADD34 protein turnover, our data provided a mechanistic basis for the high GADD34 levels seen in cells exposed to arsenite, which may contribute to the enhanced apoptosis that has been reported in response to chronic oxidative stress. In this regard, our recent studies showed that the GADD34$^{-/-}$ MEFs display significant resistance to arsenite-induced cell death, compared with WT MEFs (37).

To identify novel GADD34 functions, particularly in cells experiencing oxidative stress, we undertook mass spectrometry of anti-FLAG-GADD34 immunoprecipitates from HEK293T cells and identified eIF2α and PP1α, two known GADD34-interacting proteins (7), as well as TDP-43 and CK1ϵ, two novel GADD34 partners. In addition, our studies also identified HSP40 (38) and actin (39, 40), which had previously been shown to bind GADD34. However, other proposed GADD34-binding proteins, including PPP1R1A (41), SMAD7 (42), hSNF5/INI1 (43), LYN (44), CUEDC2 and IKK (45), Bag1 (46), TSC1/2 (47), Translin (48), CTBP2 (49), or Kif3a (50), most of which were identified by yeast two-hybrid assays, were not seen in our experiments. Unlike eIF2α and PP1α, the newly found GADD34 partners, TDP-43 and CK1ϵ bound GADD34 weakly in unstressed cells, but their association was greatly enhanced by arsenite. Consistent with arsenite eliciting a thiol-reactive oxidative stress, TDP-43 binding to GADD34 was abrogated by the antioxidant, *N*-acetylcysteine. By contrast, GADD34's association with PP1α and eIF2α was equally robust with or without stress. TDP-43 bound to an extended region of GADD34 that overlapped with the binding sites for eIF2α and PP1α (7) but did not preclude the recruitment of eIF2α and PP1α. Indeed, neither the overexpression nor siRNA-mediated knockdown of TDP-43 had any discernible impact on stress-induced GADD34 expression or GADD34-mediated eIF2α dephosphorylation (Fig. S1), suggesting that TDP-43–bound GADD34 assembled a functional eIF2α phosphatase.

GADD34 primarily associates with ER membranes, although a fraction of cellular GADD34 is also found in the cytoplasm (51). On other hand, TDP-43 is predominantly in the nucleus,

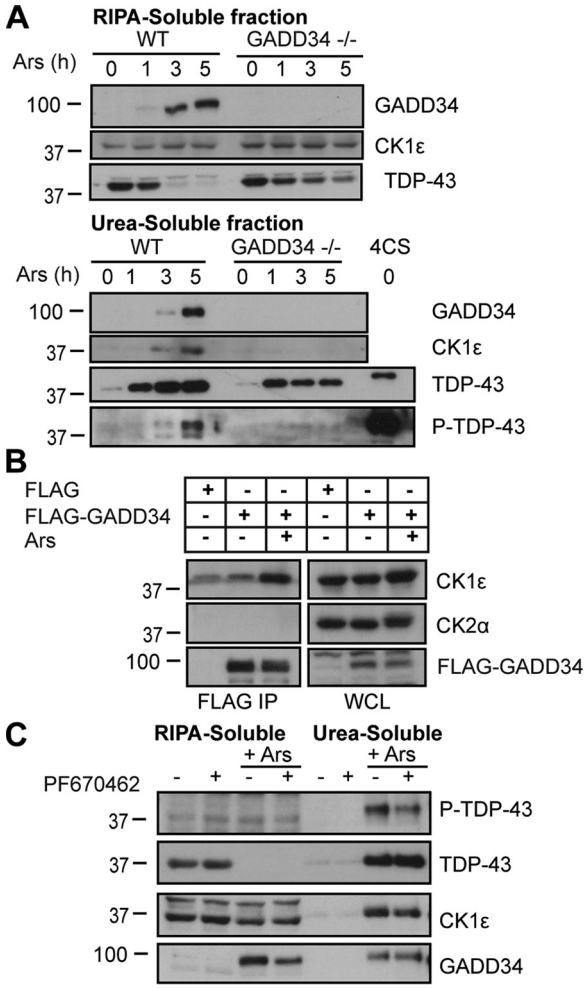

Figure 7. TDP-43 phosphorylation requires oxidative stress-mediated recruitment of GADD34 and CK1ϵ. *A*, WT and GADD34$^{-/-}$ MEFs treated with Ars (100 μM, 0–5 h) and fractionated into RIPA-soluble and urea-soluble fractions before immunoblotting for P-TDP-43, TDP-43, GADD34, and CK1ϵ. The urea-soluble fraction from HEK293T cells expressing Myc-4CS was used as a positive control for P-TDP-43. Representative data from three independent experiments ($n = 3$) are shown. *B*, HEK293T cells expressing FLAG or FLAG-GADD34 untreated or treated with Ars (0.5 mM, 1 h) were subjected to immunoprecipitation with anti-FLAG antibody, and IP and WCL were immunoblotted for FLAG-GADD34, CK1ϵ, and CK2α. Representative data from three independent experiments ($n = 3$) are shown. *C*, WT MEFs, treated with Ars (0.1 mM) along with CK1δ/ϵ inhibitor, PF670462 (1 μM), for 5 h, were fractionated into RIPA-soluble and urea-soluble fractions, which were immunoblotted for P-TDP-43, TDP-43, CK1ϵ, and GADD34. Representative data from two independent experiments ($n = 2$) are shown.

where it controls the splicing of several hundred mRNAs (52–54), including its own transcript (55). Thus, in unstressed cells, there is little likelihood of a GADD34/TDP-43 encounter (Fig. 8), and consistent with that, siRNA-mediated knockdown of GADD34 has no effect on TDP-43–catalyzed pre-mRNA splicing (Fig. S2). Following arsenite treatment, a fraction of the nuclear TDP-43 is transported to the cytoplasm, and splicing activity is partially inhibited. However, the extent of inhibition was similar in control and GADD34 knockdown cells, arguing that the nuclear functions of TDP-43 were not sensitive to stress-induced changes in GADD34. Perturbing the nucleocytoplasmic shuttling of TDP-43 by disrupting nuclear entry or export signals established that the cytoplasmic localization of TDP-43 was necessary but insufficient for GADD34 binding, as arsenite was required for GADD34 binding to ΔNLS12, a predominantly cytoplasmic TDP-43. Cysteine oxidation in TDP-43 elicited by oxidative stress (26) was mimicked by substituting serines to generate 4CS, a mutant TDP-43 that constitutively bound GADD34, highlighting the critical importance of this covalent modification for GADD34 recruitment. This characteristic was not shared by other cytoplasmic TDP-43–binding proteins, such as TIAR, whose association with WT TDP-43 and 4CS required arsenite exposure, and probably relied primarily on TDP-43 trafficking to the cytoplasm.

Prior work suggested that ALS-associated TDP-43 mutants more effectively redistributed to cytosol to be incorporated into stress granules (15). Our analyses of selected human TDP-43 mutations showed no significant difference in their association with GADD34 (Fig. S3), and similar to WT TDP-43, all of the mutant proteins displayed arsenite-induced GADD34 binding. Moreover, the loss of GADD34 function that dramatically increased the cellular content of stress granules in GADD34$^{-/-}$ MEFs in response to arsenite (Fig. S4) could be reversed by the reexpression of WT GADD34 but not by KARA, a mutant GADD34 that does not bind PP1α. This strongly suggests that GADD34 functions principally as an eIF2α phosphatase to regulate stress granule assembly (Fig. 8). Indeed, the inability of neurons to sustain stress granule assembly when experiencing chronic oxidative stress was attributed to elevated GADD34 (and CReP) expression (56). In our hands, the loss of CReP function had a modest effect on stress granule dynamics (Fig. S4), substantiating the high GADD34-mediated eIF2α phosphatase activity in arsenite-treated cells. The inability of arsenite to induce stress granules in S51A MEFs (Fig. S4) firmly established that P-eIF2α and translational repression is a critical mechanism underlying stress granule assembly and dissociated GADD34/TDP-43 binding, which was unperturbed in the S51A MEFs (Fig. 3*D*), from the control of stress granules.

Whereas some studies suggested that TDP-43 phosphorylated at serines 409/410 was recruited to stress granules (57), our studies distinguished the P-TDP-43–containing cytoplasmic puncta from stress granules by their lack of staining for TIAR (and other stress granule markers, including Caprin 1, G3BP1, eIF4E, eIF4G, and DDX6). This was particularly striking for 4CS, which was highly phosphorylated in response to arsenite (Fig. 6, *A* and *B*), but the P-4CS–containing cytoplasmic puncta displayed no stress granule markers. Phosphorylation of WT TDP-43 at serines 409/410 was preceded by the formation of urea-soluble aggregates containing HMW species and their proteolysis to 35-kDa fragments, neither of which were recognized by the phospho-TDP-43 antibody. Although the sequence of events that lead to TDP-43 aggregation, proteolysis, and phosphorylation is still unclear, our work showed that GADD34 bound TDP-43 and CK1ϵ following prolonged oxidative stress (Fig. 8). The absence of GADD34 and CK1ϵ in TDP-43–containing aggregates in arsenite-treated GADD34$^{-/-}$ MEFs provided compelling evidence in favor of a crucial role for the GADD34·TDP-43·CK1ϵ complex in TDP-43 phosphorylation, which was absent in GADD34$^{-/-}$ MEFs.

Whereas complete loss of GADD34 function is protective against oxidative stress-mediated death in a cellular model (37), the loss of one GADD34 allele in mice also improved motor

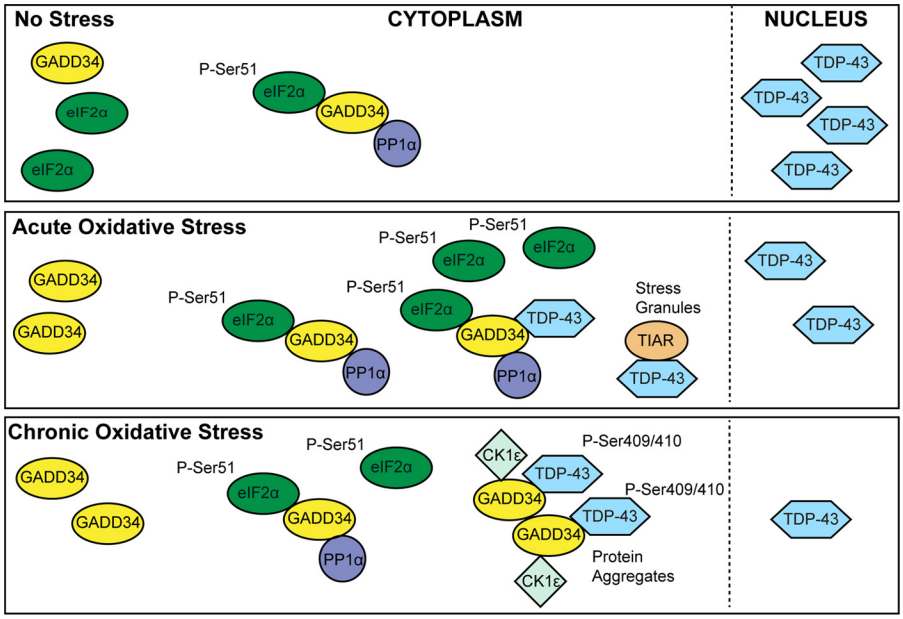

Figure 8. Roles for GADD34 in unstressed and stressed cells. *No Stress*, low, almost undetectable, levels of GADD34 are seen in unstressed cells, in which eIF2α is largely dephosphorylated. This basal GADD34 still scaffolds PP1α and eIF2α to assemble an eIF2α phosphatase that controls the translation of nearly 800 mRNAs (63). TDP-43, by contrast, is principally nuclear and controls the splicing of hundreds of mRNAs. In unstressed cells, there is little opportunity for GADD34 to encounter TDP-43. *ACUTE STRESS*, following acute or transient oxidative stress, cellular P-eIF2α levels rise, and consequently, the transcription and translation of the downstream ISR gene, *GADD34*, is also increased. The resulting increase in eIF2α phosphatase acts a feedback loop to dephosphorylate P-eIF2α and restore general protein synthesis, which had been inhibited in response to stress. Oxidative stress also promotes the redistribution of TDP-43 from nucleus to cytosol. Through its association with TIAR, TDP-43 is recruited to stress granules, stalled cytoplasmic translational complexes that can be rapidly remobilized to drive protein synthesis and cell recovery. TDP-43 also binds existing GADD34·PP1α·eIF2α complexes but does not impair their function as eIF2α phosphatases. The combined effect of eIF2α phosphorylation-dephosphorylation and stress granule dynamics facilitates cell recovery from stress. *CHRONIC STRESS*, with prolonged or chronic stress, P-eIF2α levels still remain high, but stress granules are no longer visible. The high levels of GADD34, while still assembling an eIF2α phosphatase, are now recruited to a new complex by the slow buildup of oxidized TDP-43 in the cytoplasm. This new complex, containing GADD34, TDP-43, and CK1ϵ, enhances TDP-43 phosphorylation at serines 409/410 in intracellular protein aggregates or inclusions. We speculate that this largely irreversible process of TDP-43 aggregation may deplete TDP-43 from the nucleus, compromising its nuclear functions, which may contribute to ALS and other neurodegenerative diseases (64).

function and attenuated motor neuron loss, thereby extending the lifespan of the mutant SOD1 mice (58). Our data suggest that GADD34 may assemble both as an eIF2α phosphatase to modulate ISR signaling and stress granule dynamics and a kinase complex that facilitates CK1ϵ-mediated TDP-43 phosphorylation in different temporal phases during the progression of neurodegenerative disease.

Materials and methods

Cells and transfections

HEK293T cells were cultured in RPMI 1640 medium supplemented with 10% FBS (Hyclone). HeLa cells were cultured in minimal essential medium (MEM) supplemented with 10% FBS, L-glutamine, sodium pyruvate, and MEM non-essential amino acids. HEK293T cells were cultured in DMEM with 10% FBS. MEFs were isolated from 12.5–14.5-day-old embryos from WT and GADD34$^{-/-}$ mice (59), immortalized by transfection of SV40 large T antigen, and selected by puromycin resistance. MEFs obtained from eIF2α (S51A) knock-in mice were provided by Randall J. Kaufman (Sanford-Burnham Institute). CReP null MEFs (*PPP1R15a*$^{+/-}$, *PPP1R15b*$^{-/-}$) and their genetically matched counterparts (*PPP1R15a*$^{+/-}$, *PPP1R15b*$^{+/-}$) were kindly provided by David Ron (Cambridge University). MEFs were cultured in DMEM 11995 supplemented with 10% FBS, L-glutamine, MEM non-essential amino acids, and 50 μM β-mercaptoethanol. HEK293T cells were transfected using Lipofectamine 2000 (Life Technologies) according to the manufacturer's instructions, whereas HeLa cells were transfected with FUGENE6 (Promega). Dharmafect Reagent 1 (Thermo Scientific) was used to transfect siRNAs. MEFs were transfected with plasmids using NEON electroporation (Life Technologies).

Plasmids

Plasmids expressing FLAG-tagged GADD34, 1–674, 1–620, 180–674, 1–200, and Δ2,3P and non-PP1-binding KARA mutant as well as GFP-tagged GADD34 were used as described previously (10, 22). FLAG-GADD34 1–513, 514–674, 214–513, and Δ1P constructs were cloned from pSG5-FLAG-GADD34 into pXJ40-FLAG constructs using HindIII/KpnI sites. Bacterial expression plasmids encoding GST-tagged GADD34 fragments were cloned from pXJ40 FLAG-GADD34 into pGEX4T1 constructs (GE Healthcare) via BamHI/NotI sites. The CFTR exon 9 splicing reporter plasmid, GST-TDP-43 in pGEX4T-1, FLAG-TDP-43, and RNA-binding deficient FLAG-TDP-43 (F4L) in pCMV plasmids were generously provided by Emanuele Buratti (International Centre for Genetic Engineering and Biotechnology (ICGEB), Trieste, Italy). Myc- and HA-tagged TDP-43 were generated by inserting the TDP-43 cDNA into pXJ40-Myc and pXJ40-HA, respectively, using BamHI/HindIII cleavage. Recombinant His-tagged TDP-43 protein was generated by inserting TDP-43 cDNA into pQE30 using BamHI/HindIII cleavage. Plasmids expressing Myc-TDP-

43(ΔNLS12), Myc-TDP-43(ΔNES1), and Myc-TDP-43(4CS) were obtained from Virginia M.-Y. Lee (University of Pennsylvania). Human GFP-TDP-43 expression vectors, with the ALS mutations Q331K, A315T, Q343R, and G294A, were provided by Benjamin L. Wolozin (Boston University).

Reagents

Arsenite, thapsigargin, tunicamycin, cycloheximide, N-acetylcysteine, and staurosporine were purchased from Sigma. MG132 was from Tocris, and FCCP was from Abcam. The casein kinase 1δ/ϵ inhibitor, PF670462, was provided by David M. Virshup (Duke-NUS Medical School, Singapore). These reagents were dissolved in DMSO, with the exception of arsenite and *N*-acetylcysteine, which were dissolved in water. Sources of antibodies and dilutions utilized were as follows: phospho-eIF2α (Ser-51) (Invitrogen), 1:1000; phospho-TDP-43 (Ser-409/410) (Merck Millipore), 1:1000; human-specific GADD34 (AbD Serotec, Bio-Rad), 1:500. Anti-FLAG (1:2000), anti-tubulin (1:20,000), and anti-actin (1:5000) were obtained from Sigma. Anti-CHOP and anti-hnRNPA1 1:1000 were from Cell Signaling. Antibodies against GFP, PP1α, eIF2α, mouse-specific GADD34, TDP-43, Myc, CK1ϵ, and CK2α were from Santa Cruz Biotechnology, and all were used at 1:1000 dilution. Horseradish peroxidase-linked secondary antibodies were from Santa Cruz Biotechnology and used at 1:10,000 dilution. Immunostaining and quantitation of stress granules utilized anti-TIAR (C-18, Santa Cruz Biotechnology) as well as antibodies against G3BP (BD Biosciences), eIF4E, eIF4G, DDX6, and Caprin 1 (Bethyl Laboratories). The siRNAs, GAAAGGUGCGCUUCUCCGA and GUUAACAAGUUCUCUUAUC, targeting human GADD34, siRNA CGUUCAUUCCUUAGAAAUA targeting mouse TDP-43, control siRNA, siGenome non-targeting siRNA 2, and siGenome non-targeting siRNA pool 2 were all from Dharmacon (Thermo Scientific).

Recombinant proteins

GST-GADD34 recombinant proteins were expressed in XL-1 Blue competent cells and BL21DE3 Codon Plus Gold cells, respectively, by methods described previously (41). Proteins were purified on GSH-Sepharose beads (GE Healthcare). The affinity beads were washed, and recombinant GST-GADD34 was eluted using Tris-HCl buffer, pH 8.0, containing 10 mM glutathione.

Western immunoblotting

Protein samples boiled at 95 °C for 10 min in 2× SDS sample (Laemmli) buffer (Bio-Rad) containing 5% (v/v) β-mercaptoethanol were subjected to SDS-PAGE. Polyacrylamide gels were electrophoretically transferred to PVDF membranes (Bio-Rad), incubated with 1% BSA or 5% skimmed milk in PBS or Tris-buffered saline with 0.05% Tween 20 (Bio-Rad), before immunoblotting with antibodies at 4 °C overnight. Bands were visualized with Pierce ECL or SuperSignal West Femto maximum sensitivity substrate (Thermo Scientific) on X-ray film (Fujifilm) developed using a Kodak film processor and quantified using ImageJ software.

Immunoprecipitation

Cells were lysed in 20 mM HEPES (pH 7.4) containing 137 mM sodium chloride, 1.5 mM magnesium chloride, 1 mM EGTA, 10% glycerol, 1% Triton X-100, 1 mM sodium orthovanadate, protease inhibitors (cOmplete mini EDTA-free, Roche Applied Science), and phosphatase inhibitors (PhosSTOP phosphatase inhibitor mixture tablets, Roche Applied Science). Lysates were clarified by centrifugation at 10,000 × *g* at 4 °C for 15 min, and protein concentration was estimated using Bradford reagent (Bio-Rad).

Whereas a fraction of the cell lysate was retained as whole-cell lysate (WCL), the remainder was incubated with 15 μl of M2 beads (Sigma) to immunoprecipitate FLAG-tagged proteins or 50 μl of protein G beads (Roche Applied Science) and 2 μg of monoclonal mouse anti-Myc 9E10 (Santa Cruz Biotechnology) to immunoprecipitate Myc-tagged proteins. To immunoprecipitate endogenous TDP-43, HEK293T cells (6×10^6) were treated with 100 μM arsenite for 6 h and homogenized in lysis buffer containing 0.5% (v/v) Triton X-100. The cell lysates were precleared with protein G beads (50% (w/v) slurry with lysis buffer) for 2 h at 4 °C, following which 500 μl of lysates (2 mg of total protein) were incubated with 1 μg of mouse anti-TDP-43 antibody (Santa Cruz Biotechnology) or mouse IgG for 1 h at 4 °C. Subsequently, 50 μl of fresh protein G beads were added, and the mixture was incubated overnight at 4 °C. The beads were washed three times for 10 min each at 4 °C with 500 μl of lysis buffer. The bound proteins were released with 40 μl of 2× SDS sample buffer containing 1% (v/v) β-mercaptoethanol, heated at 95 °C for 10 min, and subjected to SDS-PAGE and immunoblotting.

Protein aggregation

Cells were lysed in RIPA buffer with sonication, and total protein was quantified by a Bradford assay. Equivalent amounts of protein were subjected to centrifugation at 100,000 × *g* for 30 min at 4 °C in an Optima MAX-XP ultracentrifuge (Beckman Coulter). Supernatants defined as "RIPA-soluble fractions" were boiled in SDS sample buffer before SDS-PAGE. The pellets underwent two cycles of sonication in 100 μl of RIPA buffer followed by centrifugation. The resulting pellet was sonicated in 50 μl of urea buffer (30 mM Tris-HCl, pH 8.5, containing 7 M urea, 2 M thiourea, and 4% CHAPS). SDS sample buffer was added to the urea-extracted protein samples before SDS-PAGE and immunoblotting.

Proteomic analysis

Immunoprecipitated proteins were separated on 4–20% gradient gels (Bio-Rad) and stained with Coomassie Brilliant Blue. Regions of the gel were excised and digested with trypsin. Peptides dissolved in 3% acetonitrile, 0.1% formic acid (FA) were concentrated and desalted using a Zorbax peptide trap column (Agilent, CA) before separation on a Shimadzu UFLC capillary column containing C18 AQ (Bruker-Michrom, Auburn, CA) at a flow rate of 500 nl/min. Mobile phase A (0.1% FA in H_2O) and phase B (0.1% FA in acetonitrile) with the gradients (45 min of 5–35% B, 8 min of 35–60% B, and 2 min of 80% B) were used to elute peptides. Mass spectrometry analysis was performed in an LTQ-FT Ultra mass spectrometer (Thermo Electron, Bremen,

Germany) with an ADVANCE CaptiveSpray Source (Bruker-Michrom) to identify peptides as described previously (60). The data were submitted to the IMEx consortium (http://www.imexconsortium.org)[3] with the identifier IM-23248 and can also be accessed through IntAct (www.ebi.ac.uk/intact/) (61).

Immunostaining and image analysis

HeLa cells and MEFs grown on 18-mm glass coverslips (Assistent, Sondheim vor der Rhön, Germany) were fixed in 4% paraformaldehyde in PBS, pH 7.4 (10 min, room temperature) or methanol (5 min, −20 °C), respectively. Cells were washed with PBS containing 0.1% Triton X-100 (PBSTx) and permeabilized with 0.2% Triton X-100 in PBS for 2 min at room temperature. Coverslips were incubated with primary antibody at 1:100–200 in a humidified chamber overnight or for 2 h and washed in PBSTx and incubated with Alexa Fluor–conjugated secondary antibodies (Life Technologies) at 1:500 dilution and Hoechst 33258 at 1:1000 dilution for 1 h. Coverslips were washed with PBSTx and mounted on glass slides with FluorSave (Calbiochem) and viewed with a Carl Zeiss LSM710 microscope. All images were analyzed using ZEN software (Carl Zeiss), and quantification of stress granules, TDP-43 inclusions, and nuclei was performed using a customized MATLAB script.

CFTR splicing

CFTR exon 9 splicing was assayed using a TG(13)T(5) minigene construct as described previously (62). Total RNA was isolated from cells transfected with the minigene using RNeasy (Qiagen). 1 μg of RNA was reverse transcribed using iScript (Bio-Rad). Spliced and unspliced products, amplified by PCR with the primers Bra2 (TAGGATCCGGTCACCAGGAAGTTGGTTAAATCA) and α2-3 (CAACTTCAAGCTCCTAAGCCACTGC), were separated by electrophoresis on 1% (w/v) agarose before quantitation using Image Analyzer (Bio-Rad) or ImageJ software.

Real-time quantitative PCR

cDNAs were reverse transcribed using 1 μg of RNA using iScript (Bio-Rad) and subjected to real-time PCR using SsoFast EvaGreen Supermix (Bio-Rad) and a c1000 Touch Thermal Cycler (Bio-Rad). Quantitative PCR was performed with a 1:10 dilution of cDNA and 1 μM primers in a 10-μl reaction volume: 95 °C for 30 s, 39 cycles at 95 °C for 10 s, and 55 °C for 30 s. All samples were normalized to either β-actin or GAPDH.

Statistical analyses

Statistics were performed using GraphPad Prism version 5. One-way or two-way analysis of variance was used for analysis with Bonferroni post hoc test to calculate significance or Dunnet post hoc test to calculate significance compared with the control group. Statistical significance was expressed as follows: *, $p < 0.05$; **, $p < 0.01$; ***, $p < 0.001$.

Author contributions—The experiments were in large part conducted by C. W. G. with assistance from I. C. L., J. R. S., S. E. G., P. Y., and M. H. B. N. S. K. S. provided critical interpretations for all mass spectrometry experiments. The manuscript was written by S. S., I. C. L., and C. W. G. and has been approved by all authors.

Acknowledgments—We acknowledge the assistance of the proteomic facility at Nanyang Technological University for the mass spectrometry analyses. We also thank Tan Kia Wee, Ju Han, and Marc Fivaz for design of the MATLAB script to quantitate stress granules.

References

1. Wang, M., and Kaufman, R. J. (2016) Protein misfolding in the endoplasmic reticulum as a conduit to human disease. *Nature* **529,** 326–335 CrossRef Medline
2. Lee, Y. Y., Cevallos, R. C., and Jan, E. (2009) An upstream open reading frame regulates translation of GADD34 during cellular stresses that induce eIF2α phosphorylation. *J. Biol. Chem.* **284,** 6661–6673 CrossRef Medline
3. Palam, L. R., Baird, T. D., and Wek, R. C. (2011) Phosphorylation of eIF2 facilitates ribosomal bypass of an inhibitory upstream ORF to enhance CHOP translation. *J. Biol. Chem.* **286,** 10939–10949 CrossRef Medline
4. Vattem, K. M., and Wek, R. C. (2004) Reinitiation involving upstream ORFs regulates ATF4 mRNA translation in mammalian cells. *Proc. Natl. Acad. Sci. U.S.A.* **101,** 11269–11274 CrossRef Medline
5. Harding, H. P., Zhang, Y., Zeng, H., Novoa, I., Lu, P. D., Calfon, M., Sadri, N., Yun, C., Popko, B., Paules, R., Stojdl, D. F., Bell, J. C., Hettmann, T., Leiden, J. M., and Ron, D. (2003) An integrated stress response regulates amino acid metabolism and resistance to oxidative stress. *Mol. Cell* **11,** 619–633 CrossRef Medline
6. Rutkowski, D. T., Arnold, S. M., Miller, C. N., Wu, J., Li, J., Gunnison, K. M., Mori, K., Sadighi Akha, A. A., Raden, D., and Kaufman, R. J. (2006) Adaptation to ER stress is mediated by differential stabilities of pro-survival and pro-apoptotic mRNAs and proteins. *PLoS Biol.* **4,** e374 CrossRef Medline
7. Choy, M. S., Yusoff, P., Lee, I. C., Newton, J. C., Goh, C. W., Page, R., Shenolikar, S., and Peti, W. (2015) Structural and functional analysis of the GADD34:PP1 eIF2α phosphatase. *Cell Rep.* **11,** 1885–1891 CrossRef Medline
8. Pakos-Zebrucka, K., Koryga, I., Mnich, K., Ljujic, M., Samali, A., and Gorman, A. M. (2016) The integrated stress response. *EMBO Rep.* **17,** 1374–1395 CrossRef Medline
9. Harding, H. P., Zhang, Y., Scheuner, D., Chen, J. J., Kaufman, R. J., and Ron, D. (2009) Ppp1r15 gene knockout reveals an essential role for translation initiation factor 2 α (eIF2α) dephosphorylation in mammalian development. *Proc. Natl. Acad. Sci. U.S.A.* **106,** 1832–1837 CrossRef Medline
10. Brush, M. H., and Shenolikar, S. (2008) Control of cellular GADD34 levels by the 26S proteasome. *Mol. Cell Biol.* **28,** 6989–7000 CrossRef Medline
11. Boyce, M., Bryant, K. F., Jousse, C., Long, K., Harding, H. P., Scheuner, D., Kaufman, R. J., Ma, D., Coen, D. M., Ron, D., and Yuan, J. (2005) A selective inhibitor of eIF2α dephosphorylation protects cells from ER stress. *Science* **307,** 935–939 CrossRef Medline
12. Buratti, E., and Baralle, F. E. (2010) The multiple roles of TDP-43 in pre-mRNA processing and gene expression regulation. *RNA Biol.* **7,** 420–429 CrossRef Medline
13. Ling, S. C., Polymenidou, M., and Cleveland, D. W. (2013) Converging mechanisms in ALS and FTD: disrupted RNA and protein homeostasis. *Neuron* **79,** 416–438 CrossRef Medline
14. Colombrita, C., Zennaro, E., Fallini, C., Weber, M., Sommacal, A., Buratti, E., Silani, V., and Ratti, A. (2009) TDP-43 is recruited to stress granules in conditions of oxidative insult. *J. Neurochem.* **111,** 1051–1061 CrossRef Medline
15. Liu-Yesucevitz, L., Bilgutay, A., Zhang, Y. J., Vanderwyde, T., Citro, A., Mehta, T., Zaarur, N., McKee, A., Bowser, R., Sherman, M., Petrucelli, L., and Wolozin, B. (2010) Tar DNA binding protein-43 (TDP-43) associates with stress granules: analysis of cultured cells and pathological brain tissue. *PLoS One* **5,** e13250 CrossRef Medline
16. Hasegawa, M., Arai, T., Nonaka, T., Kametani, F., Yoshida, M., Hashizume, Y., Beach, T. G., Buratti, E., Baralle, F., Morita, M., Nakano, I., Oda, T., Tsuchiya, K., and Akiyama, H. (2008) Phosphorylated TDP-43 in frontotemporal lobar degeneration and amyotrophic lateral sclerosis. *Ann. Neurol.* **64,** 60–70 CrossRef Medline

17. Neumann, M., Kwong, L. K., Lee, E. B., Kremmer, E., Flatley, A., Xu, Y., Forman, M. S., Troost, D., Kretzschmar, H. A., Trojanowski, J. Q., and Lee, V. M. (2009) Phosphorylation of S409/410 of TDP-43 is a consistent feature in all sporadic and familial forms of TDP-43 proteinopathies. *Acta Neuropathol.* **117,** 137–149 CrossRef Medline
18. Novoa, I., Zhang, Y., Zeng, H., Jungreis, R., Harding, H. P., and Ron, D. (2003) Stress-induced gene expression requires programmed recovery from translational repression. *EMBO J.* **22,** 1180–1187 CrossRef Medline
19. Reid, D. W., Chen, Q., Tay, A. S., Shenolikar, S., and Nicchitta, C. V. (2014) The unfolded protein response triggers selective mRNA release from the endoplasmic reticulum. *Cell* **158,** 1362–1374 CrossRef Medline
20. Ma, Y., and Hendershot, L. M. (2003) Delineation of a negative feedback regulatory loop that controls protein translation during endoplasmic reticulum stress. *J. Biol. Chem.* **278,** 34864–34873 CrossRef Medline
21. Bence, N. F., Bennett, E. J., and Kopito, R. R. (2005) Application and analysis of the GFPu family of ubiquitin-proteasome system reporters. *Methods Enzymol.* **399,** 481–490 CrossRef Medline
22. Brush, M. H., Weiser, D. C., and Shenolikar, S. (2003) Growth arrest and DNA damage-inducible protein GADD34 targets protein phosphatase 1 to the endoplasmic reticulum and promotes dephosphorylation of the subunit of eukaryotic translation initiation factor 2. *Mol. Cell Biol.* **23,** 1292–1303 CrossRef Medline
23. Neumann, M., Sampathu, D. M., Kwong, L. K., Truax, A. C., Micsenyi, M. C., Chou, T. T., Bruce, J., Schuck, T., Grossman, M., Clark, C. M., McCluskey, L. F., Miller, B. L., Masliah, E., Mackenzie, I. R., Feldman, H., *et al.* (2006) Ubiquitinated TDP-43 in frontotemporal lobar degeneration and amyotrophic lateral sclerosis. *Science* **314,** 130–133 CrossRef Medline
24. Arai, T., Hasegawa, M., Akiyama, H., Ikeda, K., Nonaka, T., Mori, H., Mann, D., Tsuchiya, K., Yoshida, M., Hashizume, Y., and Oda, T. (2006) TDP-43 is a component of ubiquitin-positive tau-negative inclusions in frontotemporal lobar degeneration and amyotrophic lateral sclerosis. *Biochem. Biophys. Res. Commun.* **351,** 602–611 CrossRef Medline
25. Lu, P. D., Jousse, C., Marciniak, S. J., Zhang, Y., Novoa, I., Scheuner, D., Kaufman, R. J., Ron, D., and Harding, H. P. (2004) Cytoprotection by pre-emptive conditional phosphorylation of translation initiation factor 2. *EMBO J.* **23,** 169–179 CrossRef Medline
26. Cohen, T. J., Hwang, A. W., Unger, T., Trojanowski, J. Q., and Lee, V. M. (2012) Redox signalling directly regulates TDP-43 via cysteine oxidation and disulphide cross-linking. *EMBO J.* **31,** 1241–1252 CrossRef Medline
27. Choksi, D. K., Roy, B., Chatterjee, S., Yusuff, T., Bakhoum, M. F., Sengupta, U., Ambegaokar, S., Kayed, R., and Jackson, G. R. (2014) TDP-43 phosphorylation by casein kinase Iε promotes oligomerization and enhances toxicity *in vivo*. *Hum. Mol. Genet.* **23,** 1025–1035 CrossRef Medline
28. Arai, T., Hasegawa, M., Nonoka, T., Kametani, F., Yamashita, M., Hosokawa, M., Niizato, K., Tsuchiya, K., Kobayashi, Z., Ikeda, K., Yoshida, M., Onaya, M., Fujishiro, H., and Akiyama, H. (2010) Phosphorylated and cleaved TDP-43 in ALS, FTLD and other neurodegenerative disorders and in cellular models of TDP-43 proteinopathy. *Neuropathology* **30,** 170–181 CrossRef Medline
29. Kametani, F., Nonaka, T., Suzuki, T., Arai, T., Dohmae, N., Akiyama, H., and Hasegawa, M. (2009) Identification of casein kinase-1 phosphorylation sites on TDP-43. *Biochem. Biophys. Res. Commun.* **382,** 405–409 CrossRef Medline
30. Carlomagno, Y., Zhang, Y., Davis, M., Lin, W. L., Cook, C., Dunmore, J., Tay, W., Menkosky, K., Cao, X., Petrucelli, L., and Deture, M. (2014) Casein kinase II induced polymerization of soluble TDP-43 into filaments is inhibited by heat shock proteins. *PLoS One* **9,** e90452 CrossRef Medline
31. Andersen, P. M., and Al-Chalabi, A. (2011) Clinical genetics of amyotrophic lateral sclerosis: what do we really know? *Nat. Rev. Neurol.* **7,** 603–615 CrossRef Medline
32. Somalinga, B. R., Day, C. E., Wei, S., Roth, M. G., and Thomas, P. J. (2012) TDP-43 identified from a genome wide RNAi screen for SOD1 regulators. *PLoS One* **7,** e35818 CrossRef Medline
33. Buratti, E., and Baralle, F. E. (2009) The molecular links between TDP-43 dysfunction and neurodegeneration. *Adv. Genet.* **66,** 1–34 Medline
34. Arai, T., Mackenzie, I. R., Hasegawa, M., Nonoka, T., Niizato, K., Tsuchiya, K., Iritani, S., Onaya, M., and Akiyama, H. (2009) Phosphorylated TDP-43 in Alzheimer's disease and dementia with Lewy bodies. *Acta Neuropathol.* **117,** 125–136 CrossRef Medline
35. Schwab, C., Arai, T., Hasegawa, M., Yu, S., and McGeer, P. L. (2008) Colocalization of transactivation-responsive DNA-binding protein 43 and huntingtin in inclusions of Huntington disease. *J. Neuropathol. Exp. Neurol.* **67,** 1159–1165 CrossRef Medline
36. Jousse, C., Oyadomari, S., Novoa, I., Lu, P., Zhang, Y., Harding, H. P., and Ron, D. (2003) Inhibition of a constitutive translation initiation factor 2α phosphatase, CReP, promotes survival of stressed cells. *J. Cell Biol.* **163,** 767–775 CrossRef Medline
37. Lee, I. C., Ho, X. Y., George, S. E., Goh, C. W., Sundaram, J. R., Pang, K. K. L., Luo, W., Yusoff, P., Sze, N. S. K., and Shenolikar, S. (2017) Oxidative stress promotes SIRT1 recruitment to the GADD34/PP1α complex to activate its deacetylase function. *Cell Death Differ.* CrossRef
38. Hasegawa, T., Xiao, H., Hamajima, F., and Isobe, K. (2000) Interaction between DNA-damage protein GADD34 and a new member of the Hsp40 family of heat shock proteins that is induced by a DNA-damaging reagent. *Biochem. J.* **352,** 795–800
39. Chambers, J. E., Dalton, L. E., Clarke, H. J., Malzer, E., Dominicus, C. S., Patel, V., Moorhead, G., Ron, D., and Marciniak, S. J. (2015) Actin dynamics tune the integrated stress response by regulating eukaryotic initiation factor 2α dephosphorylation. *Elife* **4** CrossRef Medline
40. Chen, R., Rato, C., Yan, Y., Crespillo-Casado, A., Clarke, H. J., Harding, H. P., Marciniak, S. J., Read, R. J., and Ron, D. (2015) G-actin provides substrate-specificity to eukaryotic initiation factor 2α holophosphatases. *Elife* **4** CrossRef Medline
41. Connor, J. H., Weiser, D. C., Li, S., Hallenbeck, J. M., and Shenolikar, S. (2001) Growth arrest and DNA damage-inducible protein GADD34 assembles a novel signaling complex containing protein phosphatase 1 and inhibitor 1. *Mol. Cell Biol.* **21,** 6841–6850 CrossRef Medline
42. Shi, W., Sun, C., He, B., Xiong, W., Shi, X., Yao, D., and Cao, X. (2004) GADD34-PP1c recruited by Smad7 dephosphorylates TGFβ type I receptor. *J. Cell Biol.* **164,** 291–300 CrossRef Medline
43. Wu, D. Y., Tkachuck, D. C., Roberson, R. S., and Schubach, W. H. (2002) The human SNF5/INI1 protein facilitates the function of the growth arrest and DNA damage-inducible protein (GADD34) and modulates GADD34-bound protein phosphatase-1 activity. *J. Biol. Chem.* **277,** 27706–27715 CrossRef Medline
44. Grishin, A. V., Azhipa, O., Semenov, I., and Corey, S. J. (2001) Interaction between growth arrest-DNA damage protein 34 and Src kinase Lyn negatively regulates genotoxic apoptosis. *Proc. Natl. Acad. Sci. U.S.A.* **98,** 10172–10177 CrossRef Medline
45. Li, H. Y., Liu, H., Wang, C. H., Zhang, J. Y., Man, J. H., Gao, Y. F., Zhang, P. J., Li, W. H., Zhao, J., Pan, X., Zhou, T., Gong, W. L., Li, A. L., and Zhang, X. M. (2008) Deactivation of the kinase IKK by CUEDC2 through recruitment of the phosphatase PP1. *Nat. Immunol.* **9,** 533–541 CrossRef Medline
46. Hung, W. J., Roberson, R. S., Taft, J., and Wu, D. Y. (2003) Human BAG-1 proteins bind to the cellular stress response protein GADD34 and interfere with GADD34 functions. *Mol. Cell Biol.* **23,** 3477–3486 CrossRef Medline
47. Watanabe, R., Tambe, Y., Inoue, H., Isono, T., Haneda, M., Isobe, K., Kobayashi, T., Hino, O., Okabe, H., and Chano, T. (2007) GADD34 inhibits mammalian target of rapamycin signaling via tuberous sclerosis complex and controls cell survival under bioenergetic stress. *Int. J. Mol. Med.* **19,** 475–483 Medline
48. Hasegawa, T., and Isobe, K. (1999) Evidence for the interaction between Translin and GADD34 in mammalian cells. *Biochim. Biophys. Acta* **1428,** 161–168 CrossRef Medline
49. Wang, J., Huo, K., Ma, L., Tang, L., Li, D., Huang, X., Yuan, Y., Li, C., Wang, W., Guan, W., Chen, H., Jin, C., Wei, J., Zhang, W., Yang, Y., *et al.* (2011) Toward an understanding of the protein interaction network of the human liver. *Mol. Syst. Biol.* **7,** 536 Medline
50. Hasegawa, T., Yagi, A., and Isobe, K. (2000) Interaction between GADD34 and kinesin superfamily, KIF3A. *Biochem. Biophys. Res. Commun.* **267,** 593–596 CrossRef Medline

51. Zhou, W., Brush, M. H., Choy, M. S., and Shenolikar, S. (2011) Association with endoplasmic reticulum promotes proteasomal degradation of GADD34 protein. *J. Biol. Chem.* **286,** 21687–21696 CrossRef Medline
52. Tollervey, J. R., Curk, T., Rogelj, B., Briese, M., Cereda, M., Kayikci, M., König, J., Hortobágyi, T., Nishimura, A. L., Zupunski, V., Patani, R., Chandran, S., Rot, G., Zupan, B., Shaw, C. E., and Ule, J. (2011) Characterizing the RNA targets and position-dependent splicing regulation by TDP-43. *Nat. Neurosci.* **14,** 452–458 CrossRef Medline
53. Polymenidou, M., Lagier-Tourenne, C., Hutt, K. R., Huelga, S. C., Moran, J., Liang, T. Y., Ling, S. C., Sun, E., Wancewicz, E., Mazur, C., Kordasiewicz, H., Sedaghat, Y., Donohue, J. P., Shiue, L., Bennett, C. F., Yeo, G. W., and Cleveland, D. W. (2011) Long pre-mRNA depletion and RNA missplicing contribute to neuronal vulnerability from loss of TDP-43. *Nat. Neurosci.* **14,** 459–468 CrossRef Medline
54. De Conti, L., Akinyi, M. V., Mendoza-Maldonado, R., Romano, M., Baralle, M., and Buratti, E. (2015) TDP-43 affects splicing profiles and isoform production of genes involved in the apoptotic and mitotic cellular pathways. *Nucleic Acids Res.* **43,** 8990–9005 CrossRef Medline
55. Avendaño-Vazquez, S. E., Dhir, A., Bembich, S., Buratti, E., Proudfoot, N., and Baralle, F. E. (2012) Autoregulation of TDP-43 mRNA levels involves interplay between transcription, splicing, and alternative polyA site selection. *Genes Dev.* **26,** 1679–1684 CrossRef Medline
56. Shelkovnikova, T. A., Dimasi, P., Kukharsky, M. S., An, H., Quintiero, A., Schirmer, C., Buée, L., Galas, M. C., and Buchman, V. L. (2017) Chronically stressed or stress-preconditioned neurons fail to maintain stress granule assembly. *Cell Death Dis.* **8,** e2788 CrossRef Medline
57. Becker, L. A., Huang, B., Bieri, G., Ma, R., Knowles, D. A., Jafar-Nejad, P., Messing, J., Kim, H. J., Soriano, A., Auburger, G., Pulst, S. M., Taylor, J. P., Rigo, F., and Gitler, A. D. (2017) Therapeutic reduction of ataxin-2 extends lifespan and reduces pathology in TDP-43 mice. *Nature* **544,** 367–371 CrossRef Medline
58. 58 Wang, L., Popko, B., and Roos, R. P. (2014) An enhanced integrated stress response ameliorates mutant SOD1-induced ALS. *Hum. Mol. Genet.* **23,** 2629–2638 CrossRef Medline
59. 59 Patterson, A. D., Hollander, M. C., Miller, G. F., and Fornace, A. J., Jr. (2006) Gadd34 requirement for normal hemoglobin synthesis. *Mol. Cell Biol.* **26,** 1644–1653 CrossRef Medline
60. 60 Zhang, H., Guo, T., Li, X., Datta, A., Park, J. E., Yang, J., Lim, S. K., Tam, J. P., and Sze, S. K. (2010) Simultaneous characterization of glyco- and phosphoproteomes of mouse brain membrane proteome with electrostatic repulsion hydrophilic interaction chromatography. *Mol. Cell Proteomics* **9,** 635–647 CrossRef Medline
61. 61 Orchard, S., Ammari, M., Aranda, B., Breuza, L., Briganti, L., Broackes-Carter, F., Campbell, N. H., Chavali, G., Chen, C., del-Toro, N., Duesbury, M., Dumousseau, M., Galeota, E., Hinz, U., Iannuccelli, M., *et al.* (2014) The MIntAct project–IntAct as a common curation platform for 11 molecular interaction databases. *Nucleic Acids Res.* **42,** D358–D363 CrossRef Medline
62. 62 Buratti, E., and Baralle, F. E. (2001) Characterization and functional implications of the RNA binding properties of nuclear factor TDP-43, a novel splicing regulator of CFTR exon 9. *J. Biol. Chem.* **276,** 36337–36343 CrossRef Medline
63. 63 Reid, D. W., Tay, A. S., Sundaram, J. R., Lee, I. C., Chen, Q., George, S. E., Nicchitta, C. V., and Shenolikar, S. (2016) Complementary roles of GADD34- and CReP-containing eukaryotic initiation factor 2α phosphatases during the unfolded protein response. *Mol. Cell Biol.* **36,** 1868–1880 CrossRef Medline
64. 64 Kim, H. J., and Taylor, J. P. (2017) Lost in transportation: nucleocytoplasmic transport defects in ALS and other neurodegenerative diseases. *Neuron* **96,** 285–297 CrossRef Medline